Preequilibrium decay in the exciton model for nuclear potential with a finite depth

Ye. A. Bogila,[1] V. M. Kolomietz,[1,2] A. I. Sanzhur,[1] and S. Shlomo[2,3]
[1]*Institute for Nuclear Research, Kiev 252022, Ukraine*
[2]*Cyclotron Institute, Texas A&M University, College Station, Texas 77843*
[3]*The Niels Bohr Institute, 17 Blegdamsvej, 2100 Copenhagen, Denmark*
(Received 20 September 1995)

The spectra of preequilibrium particles, taking into account the energy dependence of the single-particle level density, are calculated using the particle-hole (exciton) level density. We demonstrate the significant effect of the finite depth of the potential well (continuum effect) on partial emission spectra for configurations with a small exciton number.

PACS number(s): 21.60.−n, 21.10.Ma, 23.90.+w, 27.40.+z

I. INTRODUCTION

The main element of the exciton model of preequilibrium decay [1] is the level density $\omega_n(E)$ of a nucleus in the state with excitation energy E and n excited quasiparticles (excitons). This quantity enters directly into the partial decay rates for particle emission which are obtained through the detailed balance principle. The value of $\omega_n(E)$ depends crucially on the single-particle level density $g(\varepsilon)$. Usually the assumption of a constant single-particle level density is made to obtain the density $\omega_n(E)$ in a convenient analytical form [2–6]. Some generalizations can be made by taking into account a slow dependence of $g(\varepsilon)$ on the single-particle energy ε in the vicinity of the Fermi energy [7]. These approaches provide a good approximation in the low-energy region, where the influence of the finite depth of the potential well can be neglected. However, increasing the excitation energy E leads to an increase of the partial contribution of high excited single-particle states into $\omega_n(E)$. In this case some excitons can be located in the continuum region with high probability. Discretizing the continuum, by putting the nucleus in an infinite single-particle potential well or by locating the position of the resonances, leads to a monotonically increasing single-particle level density with ε . However, for a realistic finite depth potential well, such as a Woods-Saxon potential, the value of the single-particle level density decreases with ε in the continuum region (continuum effect) [8]. Thus, a proper accounting of the continuum states, i.e., the decrease of $g(\varepsilon)$ with ε, should be taken into account in determining $\omega_n(E)$ and other quantities, especially for the case of configurations characterized by a low number of quasiparticles. The aim of this work is to investigate the influence of the finite depth of the single-particle potential on the preequilibrium decay from states with a small exciton number.

II. DECAY AND TRANSITION RATES

To estimate the influence of the finite depth of the single-particle potential on the preequilibrium decay of the nucleus we will consider the spectra for particle emission from low-exciton configurations. Within the exciton model the number of particles of ν type emitted from an n-exciton state into the energy interval de is given by

$$N_\nu(n,e)de = W_\nu(n,e)\tau_n(E)de. \tag{1}$$

Here e is the energy of the emitted particle, $W_\nu(n,e)$ stands for the particle emission rate, and $\tau_n(E)$ denotes the mean lifetime of the states having excitation energy E and $n=p+h$ excitons, where p and h are the numbers of excited particles and holes, respectively. The mean lifetime $\tau_n(E)$ is evaluated from a standard master equation [9–11] integrated over time. The early stage of the equilibration process is the most important one for the description of the preequilibrium particle emission. This stage is characterized by small exciton numbers and a predominant role of the transitions to the more complex configurations, namely, $\lambda_n^+(E) \gg \lambda_n^-(E)$, where λ_n^+ and λ_n^- are the rates for the intermediate-state transitions $n \to n+2$ and $n \to n-2$, respectively. Neglecting the terms with λ_n^- one can obtain [12,13] a simple expression for $\tau_n(E)$, namely,

$$\tau_n(E) = \tau_{n-2}(E)\lambda_{n-2}^+(E)/[\lambda_n^+(E)+\Gamma_n(E)],$$
$$\tau_{n_0}(E) = 1/[\lambda_{n_0}^+(E)+\Gamma_{n_0}(E)], \tag{2}$$

where n_0 is the initial exciton number and $\Gamma_n(E)$ is the total emission rate for the n-exciton configuration:

$$\Gamma_n(E) = \sum_\nu \int_0^{E-B_\nu} W_\nu(n,e)de. \tag{3}$$

Here B_ν is the separation energy for the emitted particle of type ν.

The main ingredient needed to obtain the quantities involved in Eqs. (1)–(3) is the level density $\omega_n \equiv \omega_{ph}$ of the excited nucleus with $n=p+h$ excitons. In particular, by applying the detailed balance principle [9], the emission rates $W_\nu(n,e)$ in Eq. (1) can be presented as

$$W_\nu(n,e) = \frac{1}{2\pi\hbar}\frac{\omega_{p-1\,h}(U)}{\omega_{ph}(E)}\sum_\ell (2\ell+1)T_\ell^{(\nu)}(e). \tag{4}$$

Here $\omega_{ph}(E)$ and $\omega_{p-1\,h}(U)$ are the particle-hole level densities for the initial and residual nuclei, respectively, and $T_\ell^{(\nu)}$ are the transmission coefficients. The excitation energy U of the residual nucleus is related to the initial excitation

energy E through the energy conservation law $E=U+B_\nu+e$. The transition rates λ_n^+ are determined by [14,15]

$$\lambda_n^+(E)=\frac{1}{\omega_{ph}(E)}\left(\int \lambda_{1p}(u)\omega_{p-1\,h}(u)\omega_{10}(u)du + \int \lambda_{1h}(u)\omega_{ph-1}(u)\omega_{01}(u)du\right), \quad (5)$$

where $\lambda_{1p}(u)$ and $\lambda_{1h}(u)$ are the probabilities per unit time of particle-particle and hole-hole scattering with the consequent creation of a particle-hole pair. The values of λ_{1p} and λ_{1h} are given by Fermi's golden rule as

$$\lambda_{1p}(u)=\frac{2\pi}{\hbar}\overline{|M|^2}\omega_{21}(u),$$

$$\lambda_{1h}(u)=\frac{2\pi}{\hbar}\overline{|M|^2}\omega_{12}(u). \quad (6)$$

Here u is the energy of an incident particle (hole) and $\overline{|M|^2}$ is the mean square of the matrix element of the residual interaction.

To determine the particle-hole level density $\omega_{ph}(E)$, let us consider an excited nucleus whose excitation energy E is shared by $n=p+h$ excitons. Under the conditions of high excitation energy and low-number quasiparticle configurations the effect of the Pauli principle can be neglected and ω_{ph} is proportional to the number of possible accommodations of p particles and h holes on the single-particle levels by the condition of energy conservation. Thus, the density $\omega_{ph}(E)$ is related to the single-particle level density $g(\varepsilon)$ as [14]

$$\omega_{ph}(E)=\frac{1}{p!h!}\int du_1\, g(\varepsilon_1)\cdots\int du_n\, g(\varepsilon_n) \times\delta\left(E-\sum_{i=1}^{n} u_i\right), \quad n=p+h, \quad (7)$$

where $u_i=\varepsilon_i-\varepsilon_F$ ($u_i=\varepsilon_F-\varepsilon_i$) is the energy of the ith particle (hole) at the corresponding single-particle level and ε_F is the Fermi energy.

To show the influence of the finite depth of the potential well on preequilibrium decay, we adopt for this purpose a finite potential well of a trapezoidal form. It has been shown [8] that for this potential well one has (i) an excellent agreement of the single-particle level density $g(\varepsilon)$ with that obtained from a corresponding Woods-Saxon well, (ii) the Thomas-Fermi approximation $g_{\rm TF}(\varepsilon)$ provides an excellent approximation to the smooth level density obtained from the exact quantum mechanical level density, and (iii) a simple analytic form for $g_{\rm TF}(\varepsilon)$ can be derived. The form of the trapezoidal potential is given by

$$V(r)=\begin{cases} V_0, & r<R-D, \\ \frac{1}{2}[1-(r-R)/D]V_0, & R-D\leqslant r\leqslant R+D, \end{cases} \quad (8)$$

where V_0, R, and D are the depth, size, and the surface thickness parameters of the potential well, respectively. Taking $V=0$ for $r>R+D$ in (8) we obtain a finite trapezoidal well with R being its half-radius. The semiclassical Thomas-Fermi single-particle level density $g_{\rm TF}(\varepsilon)$ for the potential (8) is given by [8]

$$g_{\rm TF}(\varepsilon)=\frac{1}{2\pi^2}\left(\frac{2m}{\hbar^2}\right)^{3/2}\frac{4\pi(R-D)^3}{3} \times(\varepsilon-V_0)^{1/2}\left[1+2x+\frac{8}{5}x^2+\frac{16}{35}x^3\right], \quad (9)$$

where $x=-[2D(\varepsilon-V_0)]/[(R-D)V_0]$. For the case of $\varepsilon>0$, the corresponding semiclassical expression $g_{\rm TF}(\varepsilon)$ for the finite trapezoidal potential well should be corrected by subtracting the contribution due to the free-gas level density $g_{\rm free}(\varepsilon)$ [8]:

$$g_{\rm free}(\varepsilon)=\frac{1}{2\pi^2}\left(\frac{2m}{\hbar^2}\right)^{3/2}\frac{4\pi(R+D)^3}{3} \times\varepsilon^{1/2}\left[1+2y+\frac{8}{5}y^2+\frac{16}{35}y^3\right], \quad (10)$$

with $y=-2D\varepsilon/[(R+D)V_0]$. The Fermi energy ε_F in both cases of the finite and infinite trapezoidal potential well can be determined from the conservation of the number of particles,

$$\int_{V_0}^{\varepsilon_F} d\varepsilon\; g(\varepsilon)=A,$$

where A is the number of nucleons. In the numerical calculations of (7) we have used the following parameters of the single-particle potential well [8]:

$$\begin{cases} V_0=-54+33\,t_3(N-Z)/A\ (\text{MeV}), \quad D=\pi d, \\ R=R_V/[1+(D/R)^2]^{1/3}, \quad R_V=1.12A^{1/3}+1.0\ (\text{fm}), \end{cases} \quad (11)$$

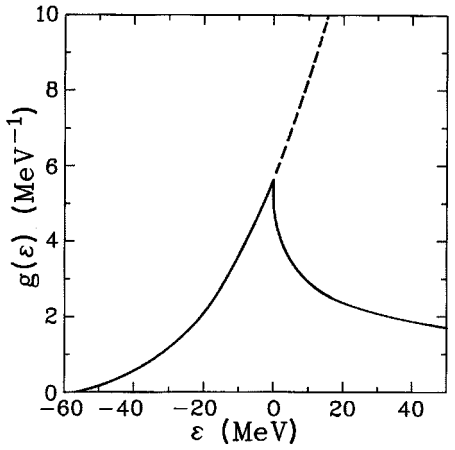

FIG. 1. The single-particle level density (protons + neutrons) as a function of energy ε for the nucleus ^{40}Ca. The dashed line is obtained using Eq. (9) for the infinite trapezoidal potential and the solid line is for the finite depth trapezoidal potential.

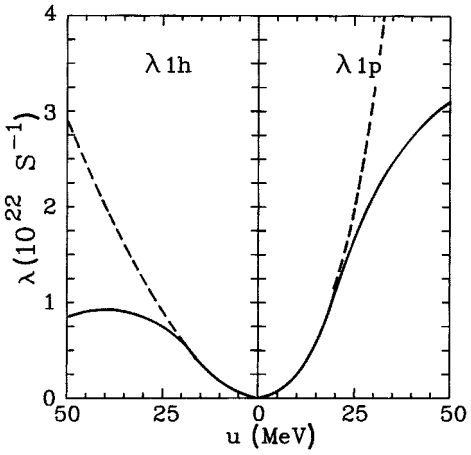

FIG. 2. The probabilities per unit time of the particle-particle (λ_{1p}) and the hole-hole (λ_{1h}) scattering accompanied with the creation of a particle-hole pair. The calculations are performed for the nucleus ^{40}Ca using Eq. (6) in the cases of a finite depth trapezoidal potential (solid line) and an infinite trapezoidal potential (dashed line).

where N and Z are the numbers of neutrons and protons, $t_3=1$ for a neutron and -1 for a proton, and $d=0.7$ fm. The value R in (11) is determined by iteration.

III. RESULTS AND DISCUSSION

We carried out numerical calculations for the cases of finite and infinite trapezoidal potential under the following assumptions.

(A) We consider only the emission of nucleons. The channels of complex particle emission are neglected.

(B) No distinction between proton and neutron is assumed. Thus, only the emission of one type of particles is considered. In contrast to the usual one-component exciton model, the contributions of protons and neutrons to the emission spectrum are taken as identical.

(C) We assume the squared matrix element of the residual interaction to be energy independent, $\overline{|M|^2}$=const. Therefore, the energy dependence of the probabilities of the exciton-exciton scattering, λ_{1p} and λ_{1h}, and the transition rates λ_n^+ are determined by the accessible phase space.

(D) Since we are basically interested in the high-energy part of the emission spectra, the transmission coefficients $T_\ell^{(\nu)}$ are approximated by the step function $\Theta(\ell-\ell_{\max})$, [16] where $\ell_{\max}\approx\sqrt{2\mu e}/\hbar$, and consequently, the sum over orbital angular momentum in Eq. (4) can be estimated as $\Sigma_\ell(2\ell+1)T_\ell^{(\nu)}(e)\approx 2\mu R^2 e/\hbar^2$, where μ is the nucleon mass. Then, for simplicity, the level densities $\omega_{p-1\,h}(U)$ and $\omega_{ph}(E)$ in (4) are calculated using the same single-particle level density $g(\varepsilon)$ of the initial nucleus.

Although the above listed assumptions are rather crude, they enable us to estimate the effect of the finite depth of the potential well on preequilibrium emission spectra. The numerical calculations have been performed for the nucleus ^{40}Ca at excitation energies $E=20$ MeV and $E=50$ MeV. Results for the case of the finite trapezoidal potential are presented in Figs. 1–4 by solid lines. In order to outline the continuum effect, the corresponding results for the infinite trapezoidal potential are displayed in the same figures by dashed lines. Figure 1 shows that the single-particle level density $g(\varepsilon)$ for the finite depth potential is a strong nonmonotonic function in the ε region close to the edge of the potential well. It decreases with ε for $\varepsilon>0$. Such behavior of $g(\varepsilon)$ underlies the effect of the finite depth of the potential well on the particle-hole level density [17] and, consequently, on the transition and decay rates. The continuum effect on the probabilities of particle-particle and hole-hole scattering is displayed in Fig. 2. Under assumption (C) the energy dependence of λ_{1p} and λ_{1h} is determined by that of the level densities ω_{21} and ω_{12}. The magnitude of the mean square of the matrix element $\overline{|M|^2}$ in Eq. (6) was taken from [18]. For ^{40}Ca we use the value of $\overline{|M|^2}=3.8\times10^{-4}$ MeV^2 which is in agreement with known parametrization [12]. As can be seen from Fig. 2, the effect of the finite depth of the potential well is to reduce the phase space accessible for the involved exciton-exciton scattering. This fact leads to the decrease of the transition rates $\lambda_n^+(E)$ with excitation energy, when compared with the results for the infinite potential well. The energy dependence of $\lambda_n^+(E)$ for the exciton configurations $2p1h$, $3p2h$, and $4p3h$ is illustrated in Fig. 3(a). In contrast to the transition rates $\lambda_n^+(E)$, the total

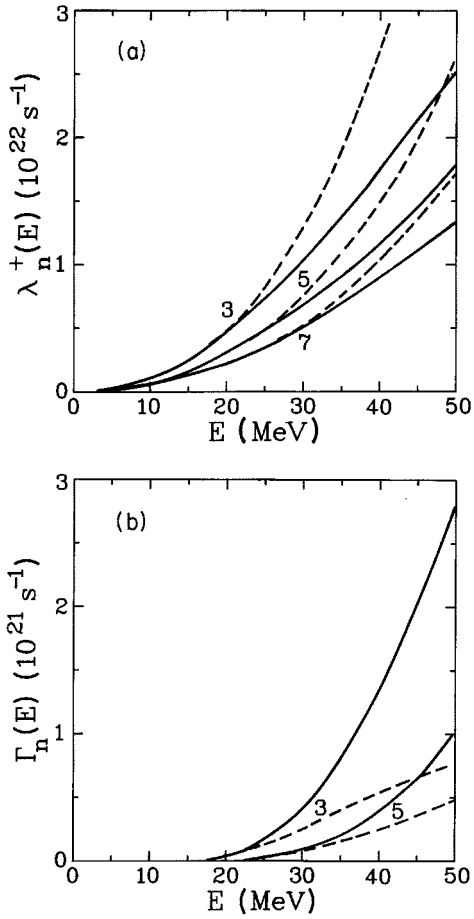

FIG. 3. The transition rates λ_n^+ (a) and the total decay rates Γ_n (b) vs excitation energy E for the nucleus ^{40}Ca. Solid lines are for a finite depth trapezoidal potential and dashed lines are for an infinite trapezoidal potential. The exciton numbers $n=p+h$ ($p-h=1$) are indicated by numerals near the curves.

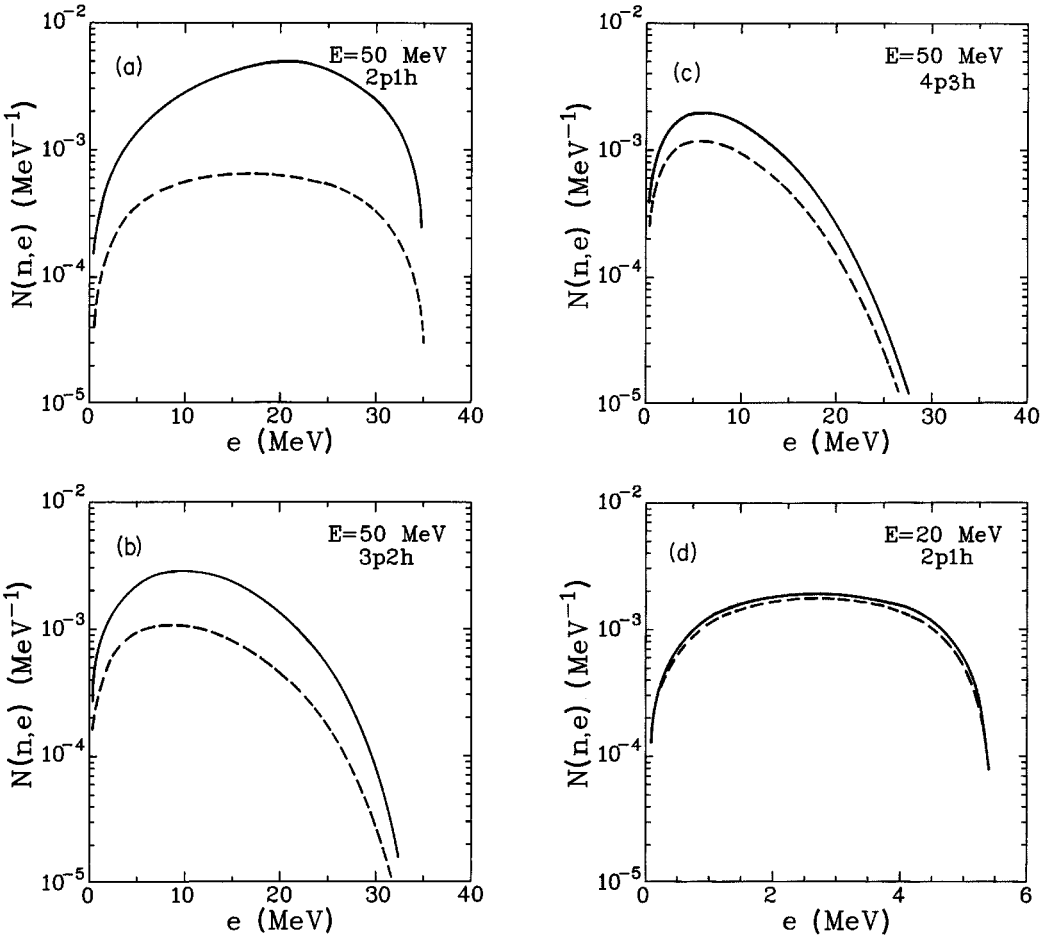

FIG. 4. Partial spectra for preequilibrium nucleon emission from low-exciton states of the nucleus ^{40}Ca at excitation energies 50 MeV (a), (b), (c) and 20 MeV (d). Dashed lines represent the calculations for the infinite trapezoidal potential; solid lines correspond to the finite trapezoidal potential. The particle-hole configurations are inserted.

decay rates $\Gamma_n(E)$, for the finite depth potential, show an increase with energy when compared with the results for the infinite potential well [see Fig. 3(b)].

To make this behavior more transparent let us analyze Eq. (4) for $W_\nu(n,e)$. When compared with the case of infinite potential well, the level density $\omega_{ph}(E)$ of the finite depth potential well is reduced significantly due to the subtraction of the free gas spectrum [17]. On the other hand, the reduction in the level density $\omega_{p-1h}(U)$ in Eq. (4) is much smaller due to the relatively small excitation energy U. Therefore, the effect of the finiteness of the potential depth leads to a rise in the emission rate $W_\nu(n,e)$ and, according to Eq. (3), in the total decay rate $\Gamma_n(E)$. As can be seen from Figs. 3(a) and 3(b), the inequality $\lambda_n^+(E) \gg \Gamma_n(E)$ is valid for both infinite and finite depth potential wells. Thus, the mean lifetimes (2) are mainly determined by the values of λ_n^+.

The results of the calculations for particle emission spectra are presented in Figs. 4(a)–4(d). These figures show that the effect of the finite depth of the potential well is more transparent when considering preequilibrium emission of nucleons at high excitation energy of the nucleus. For the case of the $2p1h$ configuration at $E=50$ MeV, taking into account the finiteness of the potential well enhances the particle yield by an order of magnitude. The difference between the spectra calculated for the finite depth potential and that for an infinite potential well becomes smaller as the exciton number increases. The same conclusion is true also for the transition and decay rates. We note that if the exciton number increases the mean value of the energy per exciton decreases. Therefore the probability for the exciton to be in the continuum ε region also decreases. As a consequence, the continuum effect tends to diminution with an increase of the exciton number. Obviously, a similar trend can be obtained by a reduction in the excitation energy of the nucleus. As can be seen from Fig. 4(d), the continuum effect at $E=20$ MeV is very small.

ACKNOWLEDGMENTS

This work was supported in part by the US National Science Foundation Grant No. PHY-9413872, the Danish Research Council, and the Soros Foundation. V.M.K. would like to thank the Cyclotron Institute at Texas A&M University for kind hospitality and S.S. thanks the Niels Bohr Institute for kind hospitality.

[1] J. J. Griffin, Phys. Rev. Lett. **17**, 478 (1966).
[2] T. Ericson, Adv. Phys. **9**, 425 (1960).
[3] F. C. Williams, Nucl. Phys. **A166**, 231 (1971).
[4] C. Kalbach, Z. Phys. A **332**, 157 (1989).
[5] E. Bétǎk, J. Dobeš, Z. Phys. A **279**, 319 (1976).
[6] C. K. Cline, Nucl. Phys. **A174**, 73 (1971).
[7] Ye. A. Bogila, V. M. Kolomietz, and A. I. Sanzhur, Z. Phys. A **341**, 373 (1992).
[8] S. Shlomo, Nucl. Phys. **A539**, 17 (1992).
[9] C. K. Cline and M. Blann, Nucl. Phys. **A172**, 225 (1971).
[10] C. K. Cline, Nucl. Phys. **A193**, 417 (1972).
[11] I. Ribanský, P. Obložinský, and E. Běták, Nucl. Phys. **A205**, 545 (1973).
[12] K. Seidel, D. Seeliger, R. Reif, and V. D. Toneev, Fiz. Elem. Chastits At. Yadra **7**, 499 (1976) [Sov. J. Part. Nucl. **7**, 192 (1976)].
[13] J. Dobeš and E. Běták, Z. Phys. A **288**, 175 (1978).
[14] E. Gadioli, E. Gadioli Erba, and P. G. Sona, Nucl. Phys. **A207**, 589 (1973).
[15] P. Obložinský, I. Ribanský, and E. Běták, Nucl. Phys. **A226**, 347 (1974).
[16] G. Goldstein, in *Fast Neutron Physics*, edited by J. B. Marion and J. L. Fowler (Atomizdat, Moscow, 1966), Vol. 2, Chap. 10, p. 386.
[17] S. Shlomo, Ye. A. Bogila, V. M. Kolomietz, and A. I. Sanzhur, Z. Phys. A **353**, 27 (1995).
[18] Ye. A. Bogila, V. M. Kolomietz, and A. I. Sanzhur, Yad. Fiz. (to be published).